diversity

MDPI

Article

Intra-Annual Course of Canopy Parameters and Phenological Patterns for a Mixed and Diverse Deciduous Forest Ecosystem Along the Altitudinal Gradients Within a Dam Reservoir Landscape

Melih Öztürk [1,*], Turgay Biricik [1] and Ali Vasfi Ağlarcı [2]

[1] Department of Landscape Architecture, Division of Landscape Techniques, Faculty of Engineering, Architecture and Design, Bartın University, Room No: 314, Ağdacı Campus, 74110 Bartın, Türkiye; turgaybiricik@gmail.com

[2] Department of Biostatistics, Faculty of Medicine, Kuzeykent, Kastamonu University, 37150 Kastamonu, Türkiye; alivasfi.aglarci@kastamonu.edu.tr

* Correspondence: melihozturk@bartin.edu.tr; Tel.: +90-378-223-38-42

Abstract: Within a dam reservoir landscape in the Western Black Sea Region of Türkiye, a dense young-mature stand composed diversely of oriental beeches, European hornbeams, sessile oaks, and silver lindens was chosen as a study field to analyze canopy parameters and to determine phenological patterns along the altitudinal gradients. Referring to the air-soil temperature and precipitation data, intra-annual eco-physiological characteristics of that stand tree canopies, were aimed to be determined regarding those altitudinal gradients. For each of the 10 altitudinal gradients, the mixed deciduous stand canopy physiological characteristics were analyzed by hemispherical photographing. Canopy parameters were acquired from those digital hemispherical photographs, which were confirmed with secondary LAI data from the LAI-2200C. Leaf Area Index, Light Transmission, Canopy Openness, and Gap Fraction were obtained during a total of 21 study field visits throughout the monitoring year. Beginning from a theoretical leafless stage with 0.51 m^2 m^{-2}, average LAI increased to 0.89 m^2 m^{-2} during budburst stage, and then gradually up to 3.60 m^2 m^{-2} during climax leaf period, and then to 1.38 m^2 m^{-2} during senescence period, and gradually down to 0.50 m^2 m^{-2} during the next theoretical leafless stage. However, average LT (64%, 61%, 9%, 36%, 74%), CO (65%, 62%, 9%, 37%, 75%), and GF (18%, 14%, 1%, 8%, 14%) followed opposite patterns. Though no apparent trend was valid for those canopy parameters from the lowest to the highest altitudinal gradient, their obvious intra-annual patterns emerged as compatible with the annual air-soil temperature data course.

Keywords: landscape ecology; tree eco-physiology; tree diversity; LAI; elevation zones; air-soil temperature; Kirazlıköprü dam watershed

check for updates

Academic Editor: Mario A. Pagnotta

Received: 3 March 2025
Revised: 21 April 2025
Accepted: 26 April 2025
Published: 4 May 2025

Citation: Öztürk, M.; Biricik, T.; Ağlarcı, A.V. Intra-Annual Course of Canopy Parameters and Phenological Patterns for a Mixed and Diverse Deciduous Forest Ecosystem Along the Altitudinal Gradients Within a Dam Reservoir Landscape. *Diversity* **2025**, *17*, 331. https://doi.org/10.3390/d17050331

Copyright: © 2025 by the authors. Licensee MDPI, Basel, Switzerland. This article is an open access article distributed under the terms and conditions of the Creative Commons Attribution (CC BY) license (https://creativecommons.org/licenses/by/4.0/).

1. Introduction

After the construction of stream dams, running streams become still water as they come close to the body of the dams. Therefore, the upstream sections of the reservoirs that are close to their dams usually generate wide water surfaces in the form of lakes. Hence, these dam lakes often constitute harmonious composition with their upstream environments within rural landscapes. Nevertheless, this harmonious composition not only has an aesthetic dimension but also has an ecological aspect, which particularly involves nutritional, meteorological, and hydrological exchanges between these dam lakes and their

surrounding ecosystems [1]. Thus, their upstream surrounding ecosystems may include forests, grasslands, and even undesirable farms, or their coexistence within those rural landscapes. However, within these surrounding ecosystems, existence and maintenance of a relatively natural environment is necessary to sustain the physical and chemical quality of these dam lakes [2]. Therefore, forest or woodland ecosystems surrounding the upstream dam lakes are more advantageous in favor of supporting better-quality groundwater that feeds these dam lakes [3]. In addition, these surrounding forest and woodland ecosystems also diminish direct rainfall. As such, overland flow that eventually leads into the dam lakes decreases, which positively contributes to the regulation of the stream and lake water regime. Hence, diverse canopies of the trees and shrubs, together with their trunks, branches, and litterfall, prevent water erosion. Nonetheless, excessive sediment and nutrient loading into these dam lakes, which reduces the water storage capacity of the reservoirs and is associated with expiry of the dam lakes, will also be prevented [4]. On the other hand, water bodies such as dam lakes tend to provide milder temperatures and tend to moderate local climate for their surrounding ecosystems [5]. In return, forest and woodland ecosystems supply shade on those water bodies, particularly by means of their diverse canopies. Thus, they preserve these water bodies to become warmer and to lose much water by evaporation [6].

Ultimately, forest and woodland ecosystems surrounding the upstream environment of the dam lakes support the soil and water conservation within the overall landscape. Hence, these natural ecosystems ensure the sustainability of the dam lakes together with their environment. However, there are many bio-meteorological [7], eco-physiological [8], hydro-geological [9], and pedo-topographical [10] factors that directly or indirectly affect the degree of this conservation and influence the level of that sustainability. Out of those integrated factors, air-soil temperature, tree phenology-physiology, and hillside altitude are the prominent ones. In fact, they principally influence the ecological role of forest and woodland ecosystems on those dam lakes. Conversely, construction of the dams and establishment of their upstream lakes also affect these forest and woodland ecosystems' air-soil temperature and tree phenology-physiology. The primary reason for this situation is the cooling and warming effect of their repeatedly deposited water [11]. Therefore, monitoring and analyses of these climatical, phenological, and physiological factors will determine the causes of further possible changes in the quantity and quality of the dam lake waters. In addition, their monitoring and analyses will identify the reverse effects of these waters, which these factors may probably experience [12]. Indeed, since the air-soil temperature and tree phenology-physiology vary temporally, their monitoring and analyses should be frequently conducted all year round as well as across multiple years. Thus, their seasonal, inter-seasonal, and monthly transitions can be distinguished to represent the overall surrounding forest and woodland ecosystem within the dam lake landscape. On the other hand, detecting the correlations of air-soil temperature and hillside altitude with tree phenology-physiology is significant. This is because this detection allows us to indicate the degree of climatological and topographical influences on the intra/inter-annual phenological-physiological changes of the forest and woodland tree species [13].

Amongst the phenological and physiological characteristics of the forest and woodland tree species, canopy characteristics are the most determinant factors on the dam lakes. Nonetheless, their canopies are also the most directly affected characteristics, being highly influenced by the ecological factors, particularly by the air-soil temperature [14] and hillside altitude [15]. Parameters that define both the phenological and physiological canopy characteristics of the forest and woodland tree species are relatively restricted within the scientific literature. Leaf Area Index (LAI, m^2 m^{-2}) defines the average projected one-sided area of the leaves over the canopy-covered ground area [16]. Therefore, it is a

key canopy index for parameterizing many ecological, hydrological, and physiological processes within an ecosystem [17–19]. On the other hand, and directly associated with LAI, Light Transmission (LT, %) and Canopy Openness (CO, %) are the two other interconnected canopy parameters. LT defines the amount of light that penetrates through the canopy [20] whereas Canopy Openness (CO) defines the pathways of that light throughout that canopy. Hence, Gap Fraction (GF, %) defines the proportion of the openness over the ground area that is covered by that canopy. Although LAI varies according to many factors, such as tree species and diversity, the seasonal, inter-seasonal, and monthly development of this canopy parameter is directly influenced by weather conditions [21]. In addition, LT, CO, and GF are all correlated parameters that the canopy structure, diversity, and other characteristics predominantly affect [22].

Consequently, in this study, regarding its altitudinal gradients, we used these canopy parameters to address some phenological and physiological characteristics of a forest stand on a hillside near a dam lake. Diverse canopies of this stand composed of homogenously mixed deciduous tree species could be monitored and analyzed at this dam lakeside hill. Before the construction of the dam, this hillside had been within the riparian zone of the stream (Figure 1). The homogeneously mixed deciduous stand was chosen as the sample research field on the dam lakeside hill to best represent the diversity of the overall canopies of the surrounding forest ecosystems within the entire rural landscape. As a matter of fact, the aim of this study is to determine some canopy phenological and physiological characteristics of this homogenously mixed deciduous stand by monitoring and analysis of the canopy parameters. Along the altitudinal gradients throughout a whole year, these monitored and analyzed basic parameters are LAI, LT, CO, and GF. In accordance with this purpose, the monitoring and analysis procedures involved both digital hemispherical photographing and on-site canopy analyzing with LAI-2200C device at certain fixed points under the diverse tree canopies of the gradual altitudes on the hillside near the dam lake. For the sake of regarding all the intra-annual phenological stages and distinguishing the transitions among them, these monitoring and analysis processes were conducted by performing more frequent field visits between the late winter and early summer. However, infrequent field visits were performed until the end of the following year's winter. Thus, particular attention would be paid to discover not only the seasonal but also the inter-seasonal phenological and physiological characteristics of the mixed and diverse deciduous tree canopies. Hence, their diverse canopies might have probably influenced the quantity and quality of this dam lake. Thereafter, digital hemispherical photographs were analyzed using image processing software for the purpose of obtaining temporally variable and spatially diverse LAI, LT, CO, and GF parameter data. Nevertheless, the secondary LAI data were obtained by the LAI-2200C device for their comparison and control. Ultimately, statistical analyses were applied for all canopy parameters data to understand the existence and significance of their correlation either with the air-soil temperature data or with the hillside altitudinal gradients.

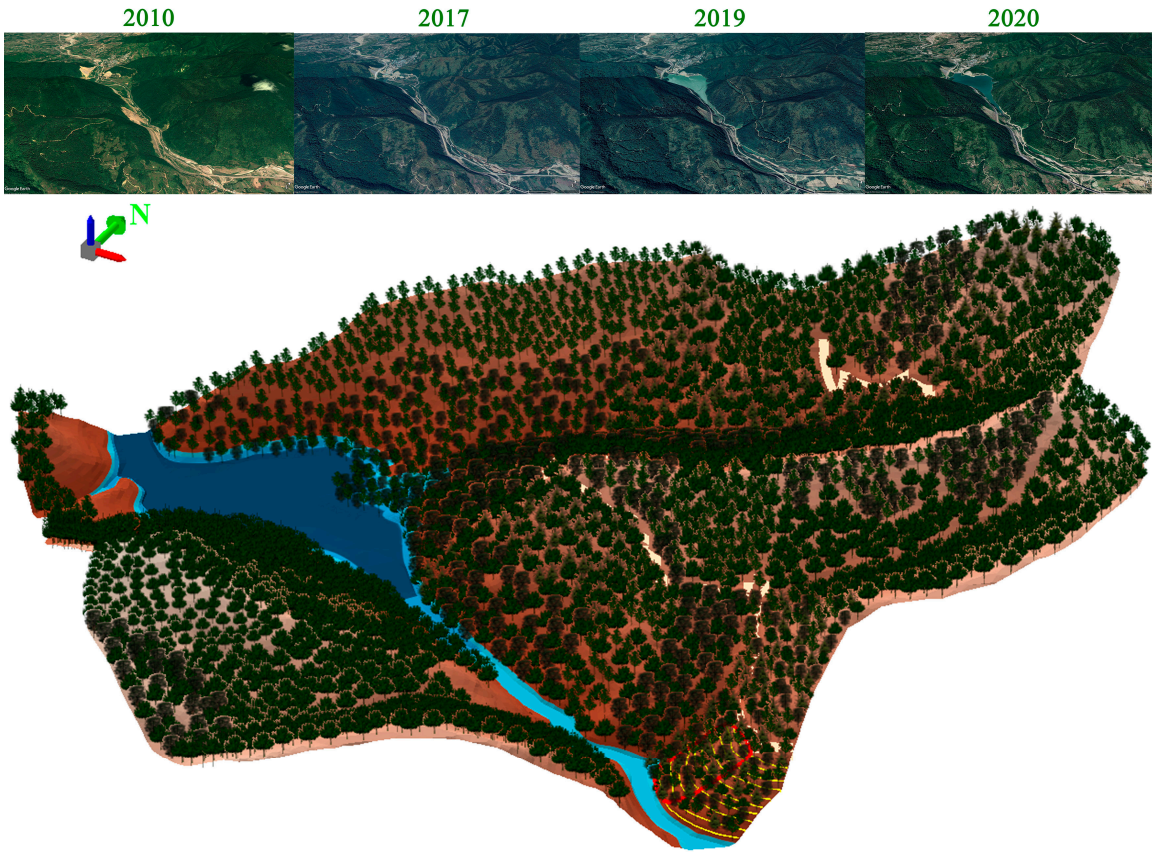


Figure 1. Above: Images following the first construction of the dam, displaying cut-and-fill applications within the riparian zone of the stream channel before (2010–2017) and after (2019–2020) the occurrence of reservoir water or lake. **Below:** Three-dimensional simulation and illustration of Kirazlıköprü dam reservoir landscape (with 13.3 km perimeter and 10.8 km^2 area) consisting of lake (hues of blue), forest ecosystems, and road (thick sand beige line).

2. Materials and Methods

2.1. Overall Dam Reservoir Landscape Characteristics

The construction of the Kirazlıköprü dam started in 1999. The dam is approximately 17 km away from the Bartın city center [23]. A landscape border extending to a perimeter of about 13.3 km and overspreading an area of about 10.8 km^2 was delineated for the closer reservoir (Figure 1). Being 325 m asl. on average, the altitudes of the dam reservoir landscape range from 60 m to 740 m asl. The closer reservoir floor and main body of the dam lies at the lowest altitude whereas the top of the highest hill represents the highest altitude within the surrounding landscape (Figure 2). Average perimeter and area of the closer reservoir or lake surface are 8 km and 1 km^2, respectively, principally alternating with precipitation and flood (Figures 1 and 3). According to the long term (between years 1975 to 2021) meteorological data, the average annual temperature is 11.9 °C and the average annual total precipitation is around 1050 mm [24]. The precipitation primarily falls as rain in all seasons, though it also falls as snow in winter and early spring [24]. As such, the region falls into the mesothermal humid climate regime [25].



Figure 2. Instant digital compact photograph of part of the dam reservoir landscape during winter (**bottom**). Also, the location of the study field (minor red polygon-**middle/right** map) together with the hemispherical photographing points (yellow landmarks-**middle/right** map) within the dam reservoir landscape with green vegetation cover (major red polygon-**middle/left** map) and altitudinal gradients (gradual shades of earth-**middle/right** map). In addition, the location and altitudinal gradients of the Kirazlıköprü dam watershed (gradual shades of earth-**top/right** map) within the Western Black Sea Region of Türkiye (**top/left** map).

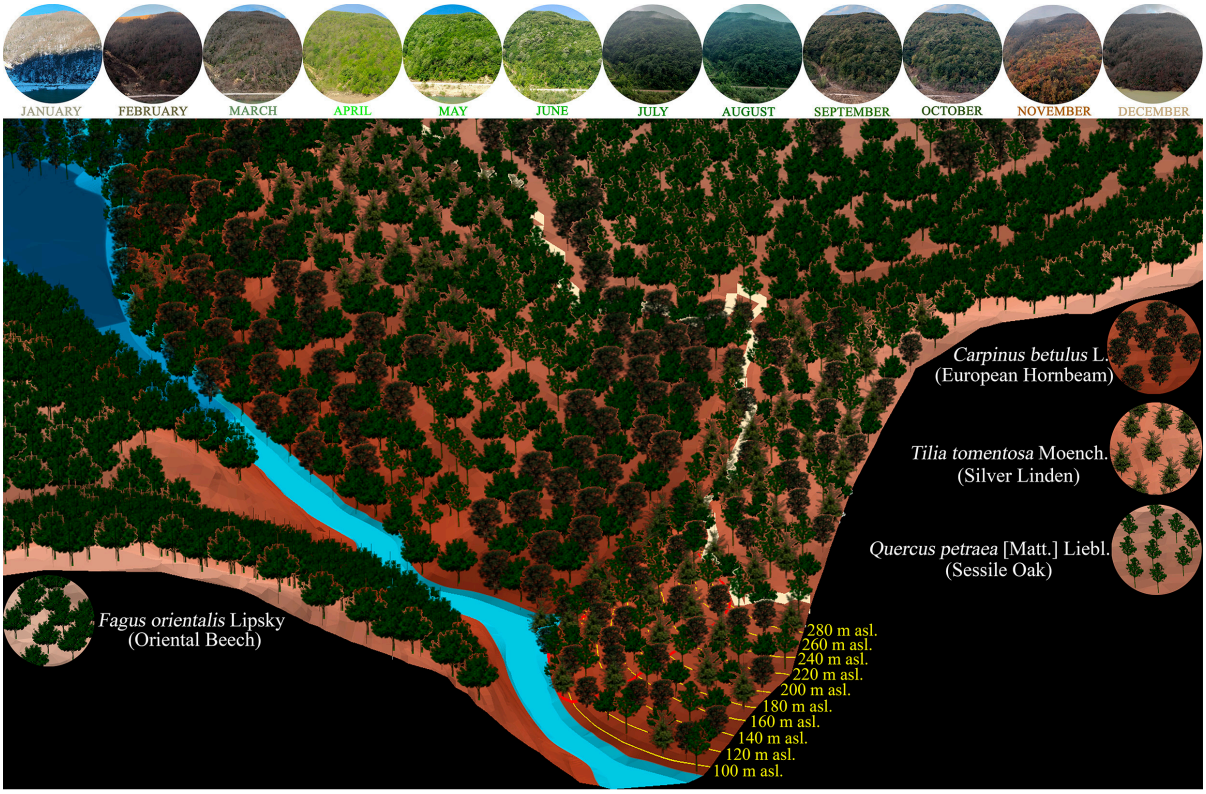


Figure 3. Above: Real successive monthly focal terrain images of the study field with immediate surroundings, taken by instant compact photographs at the opposite hill with a bird's eye distance of average 200 m. **Below**: Simulation and illustration of part of the Kirazlıköprü dam reservoir landscape focusing primarily on the study field together with the representative tree species (with their focal images), altitudinal gradients (*thin yellow lines and numbers*), and forest road (*thick sand beige line*).

The overall dam reservoir landscape consists of various deciduous pure and mixed forest stands [26]. These stands involve diverse tree species and canopies with different dense (canopy closure ≥71%) and sparse (canopy closure ≤70%) closures [26]. Those diverse tree canopies are composed of four dominant species: sessile oak (*Quercus petraea* [Matt.] Leibl.), European hornbeam (*Carpinus betulus* L.), oriental beech (*Fagus orientalis* Lipsky), and silver linden (*Tilia tomentosa* Moench.) [26] (Figure 3). The various pure stands include dense compositions of young beeches, dense and sparse compositions of mature beeches, and dense compositions of mature sessile oaks (Figures 1 and 3). On the other hand, the various mixed stands include diverse dense and sparse compositions of both young and mature trees of European hornbeam with oriental beech, mature trees of oriental beech with silver linden, and mature trees of oriental beech with sessile oak (Figures 1 and 3). In addition, these various mixed stands also include diverse dense compositions of both young and mature trees of European hornbeam with sessile oak (Figures 1 and 3). Furthermore, two sparse forest stands are composed of all four of those deciduous tree species within this dam reservoir landscape (Figures 1 and 3). These sparse stands include a mixture of young European hornbeams with young oriental beeches with mature sessile oaks, and with mature silver lindens. However, they are divided by the forest road passing through them (Figures 1 and 3). In fact, our study field was delineated within the altitudinal lower of these last two sparse stands (Figures 1 and 3).

2.2. Study Field Characteristics

The study field is at the eastern side of the dam reservoir landscape (Figure 2). It is situated between the forest roads (Figure 2). It is located between the 41°31′29″ and 41°31′41″ northern latitudes and between the 32°30′24″ and 32°30′39″ eastern longitudes. The field covers approximately 7.6 ha with a perimeter of about 1 km (Figure 2). The altitude of the study field ranges between 100 m and 280 m asl., being 190 m asl. on average. The average slope is 29°, indicating a relatively steep slope for this field (Figures 2 and 3). The dominant aspect of the field is southwest, and the dominant northeaster wind blows towards the southwest direction [24]. The very shallow (0–20 cm) limeless brown forest soils [27] have formed on sandstone-mudstone geological formations [28] within the study field. A forest road serves the forest stands at higher altitudes. It is over the north-eastern border of this study field, and it passes along the immediate top of this border (Figures 1–3). The dominant vegetation cover within the study field is homogeneously composed of four deciduous tree species. They are sessile oaks (*Quercus petraea* [Matt.] Leibl.), European hornbeams (*Carpinus betulus* L.), oriental beeches (*Fagus orientalis* Lipsky), and silver lindens (*Tilia tomentosa* Moench.) (Figure 3). Indeed, according to the district-based forest management plan and report of The Turkish General Directorate of Forestry, this homogenous mixed deciduous stand involves these trees of diverse species but of the same age, as indicated with their mean DBH [26]. Thus, the mean DBH (Diameter at Breast Height) and height of the young European hornbeams and young oriental beeches are 14 cm and 25 m, respectively [26]. On the other side, the mean DBH and height of the mature sessile oaks are 28 cm and 25 m [26]. The mean DBH and height of the mature silver lindens are 44 cm and 29 m [26]. Although mixed stands are generally composed of two tree species, this study field is composed of four tree species, revealing the species diversity. Hence, the general physiological and ecological characteristics of these diverse deciduous tree species present their harmonious composition and coexistence. As a matter of fact, both the sessile oak and oriental beech are members of the Fagaceae family, whereas European hornbeam and silver linden belong to the Betulaceae and Tiliaceae families, respectively. The leaves of sessile oak and oriental beech are both elliptic and obovate-oblong, whereas the leaves of the European hornbeam and silver linden ovate and acuminate [29]. The reddish-brown shoots are also common to the sessile oak, European hornbeam, and oriental beech [29]. The barks of the European hornbeam, oriental beech, and silver linden are all grey and smooth, whereas sessile oak has a longitudinal deep-cracked mature trunk with light grey-brown bark [30]. Representing the common characteristics of their ecosystems, all these four tree species extend from Europe towards Northern Anatolia, Türkiye [31–33]. Sessile oak and silver linden are direct sunlight-demanding tall trees, whereas tall oriental beech and medium-height European hornbeam are shade-tolerant tree species [34]. All four of these tree species can establish healthy stands within the temperate and humid forest ecosystems [35]. Nonetheless, the poor adaptation of sessile oak to cold climates and oriental beech to drought makes it necessary for them to be under the protection of the European hornbeam and silver linden, particularly because of the latter's resistance to the extreme climate conditions, including cold climates [36].

2.3. Methodology

2.3.1. Hemispherical Photographing, LAI-2200C and Analyses

Within the study field, to determine the intra-annual phenological and physiological characteristics of the mixed forest stand composed of the previously mentioned four diverse deciduous tree species, the technique that integrates taking hemispherical photographs and their image analyses was applied. Moreover, for the confirmation of the LAI data, in-situ analyses were performed with another LAI device. For this purpose, ranging with 20 m

intervals between 100 m and 280 m asl., 10 different altitudinal gradients were chosen on the slope of this study field (Figures 2 and 3). Thus, three hemispherical photographing and in-situ LAI analysis points were defined on the field and marked with sign boards for each of these altitudinal gradients. Therefore, this definition accounted for 30 hemispherical photographing and analysis points in total (Figure 2). Hemispherical photographs (180°) of the tree canopies were taken on these fixed points. An 8 mm fisheye objective (Sigma F3.5 EX DG Circular Fisheye-Sigma Corporation, Kanagawa, Japan) was mounted on a digital camera (Canon EOS 5D SLR digital camera-Canon Inc., Tokyo, Japan). Using the LAI-2200C Plant Canopy Analyzer device (LI-COR Biosciences Inc., Lincoln, NE, USA), LAI data were obtained in-situ. During the field work, the hemispherical photographing procedure beneath these diverse tree canopies was conducted. Indeed, this montage photographing equipment was held perpendicular (90°) to the ground plane and it was focused toward those canopies above. The LAI device was also used to analyze the in-situ, instantaneous, and immediate LAI values. Monitoring all the phenological stages of those diverse tree canopies were addressed in this study. Beginning from their budding period and ending with their completely theoretical leafless period, 21 field visits were conducted during the year-round monitoring period (Figure 3). These field visits, with each of their 30 photographs and in-situ device outcomes (Figure 2), accounted for 630 hemispherical photographs and in-situ LAI values as the overall total. Indeed, almost weekly frequent field visits were conducted from the bud formation of these deciduous trees in early-March until their practically full foliation in late-May. This frequent monitoring accounted for 12 visits. Then, almost monthly infrequent field visits were conducted from that term of fully foliated trees in early-June until their theoretically bareness in late-February. This infrequent monitoring accounted for the remaining nine visits (Figure 3). The digital images of these 630 hemispherical photographs were initially categorized according to their altitudinal gradients. They were also classified based on their field visit dates. Then, they were introduced to the image analyses and processing program, Hemisfer version 3.1 (Swiss Federal Institute of Forest, Snow and Landscape Research, [37]). The LAI data from the LAI-2200C Plant Canopy Analyzer device (Biosciences Inc., Lincoln, NE, USA) were also categorized and classified according to their altitudinal gradients and field visit dates. These LAI data were then used not only to verify the LAI data from the Hemisfer version 3.1, but also for joint usage with them. Indeed, they were both used during the determination of the phenological and physiological characteristics of the mixed and diverse deciduous tree canopies. They were also used for further correlation with the meteorological variables. As a result of the analyses of the hemispherical photograph images with Hemisfer 3.1, the canopy parameters of LAI, LT, GF, and CO were obtained based on distinguishing between sky and canopy pixels [37]. During the analyses, the methodology of the LAI-2000 was compulsorily preferred for compatibility with the LAI-2200 device. The methodology of the automatic thresholding was applied according to the study by the authors of [38]. The integrated methodology, based on the studies by the authors of both [37,39], was referred to during the necessary corrections for the analyses.

2.3.2. Meteorological Data of the Dam Reservoir Landscape

There was no immediate meteorological station within or around the dam reservoir landscape. Thus, adaptation and modification processes were applied for the air-soil temperature and precipitation data from the Bartın meteorological station. Nevertheless, the validity of these processes was ensured by depending upon the high correlation (r = 0.911) between the Bartın (36 m asl.) and Ulus (186 m asl.) meteorological stations for the data spanning 10 years (2012–2021). Furthermore, confirming this high correlation and indicating the initial lapse rate, the average air temperature of the former station is approximately

1.0 °C higher than the average of the latter at the higher altitude. The Ulus meteorological station is just 15 km away from the study field. The more regular existence and consistence of the meteorological data, particularly the soil temperature data of the Bartın meteorological station, led this study to prefer them rather than those of the closer Ulus meteorological station. On the other hand, due the difference in altitude and, accordingly, the temperature between the Bartın meteorological station and the study field, the lapse rate was referred to for the adaptation and modification of the air-soil temperatures. Therefore, the lapse rate was principally accepted to be −0.5 °C/100 m, as suggested by scientific literature for such as this mesothermal humid region [40]. In addition, based on that altitudinal difference, the precipitation difference was principally accepted as +54 mm/100 m [40]. Hence, the mean daily air-soil temperature differences between these two locations were assumed to be −1.0 °C and +108 mm, respectively. Then they were adapted, modified, and conveyed for the subsequent calculations. Then, temperature and precipitation data for the one week prior to the first monitoring were also initially considered. Afterwards, the adapted-modified mean air-soil temperature and total precipitation data were calculated for the intervals between each of those frequent and infrequent field visits of hemispherical photographing. These interim adapted-modified mean air-soil temperature and total precipitation data were then referred to for both the meteorological interpretation of the results on the canopy parameters during the phenological periods and for their correlation analyses with those canopy parameters.

2.3.3. Statistics and Correlations with Meteorological Variables

To clearly define the influence of the temperature and precipitation on the intra-annual course of canopy parameters of the mixed and diverse deciduous forest trees, correlation and significance analyses were conducted between these meteorological data and the canopy parameters data. Thus, using the SPSS software, version 20.0 (SPSS Inc., Chicago, IL, USA), Spearman correlation and significance tests were conducted [41]. For this purpose, the adapted-modified mean air-soil temperature and total precipitation data during each of the 21 field visit intervals were subjected to the Spearman correlation and significance tests with their mean canopy parameter values. These field visits covered the monitoring period beginning from early spring in 2021 and finishing in late winter in 2022. For the sake of inquiry, the previous year's (2020–2021) total precipitation data, which coincide with the intervals of the same periods of the current year (2021–2022), were also included in those statistical analyses. Then, all these Spearman correlation and significance test results were tabulated in the form of a matrix (Table 1). This matrix includes the previous and current years' precipitation data together with the air and soil temperature data that involve −5 cm, −10 cm, −20, −50 cm, and −100 cm depths, all representing one side of the two axes (Table 1). Accordingly, the intra-annual data of the forest tree canopy parameters represent the other side of the two axes (Table 1). Hence, the intra-annual course of the eco-physiological characteristics of these forest tree canopies would have been determined in terms of LAI, LT, CO and GF parameters.

Table 1. Spearman correlations (*r*) of mean adapted-modified air-soil temperature data, mean adapted-modified total precipitation data with average LAI, LT, CO, GF data for all altitudinal gradients, together with their significance (*p*) at 0.01 ** level.

	LAI (m^2 m^{-2})	LT (%)	CO (%)	GF (%)
Air Temperature (°C)	***r* = 0.894 ** *p* = 0.000**	***r* = −0.935 ** *p* = 0.000**	***r* = −0.935 ** *p* = 0.000**	***r* = −0.887 ** *p* = 0.000**
Soil Temperature (°C, −5 cm)	***r* = 0.930 ** *p* = 0.000**	***r* = −0.969 ** *p* = 0.000**	***r* = −0.969 ** *p* = 0.000**	***r* = −0.923 ** *p* = 0.000**
Soil Temperature (°C, −10 cm)	***r* = 0.922 ** *p* = 0.000**	***r* = −0.968 ** *p* = 0.000**	***r* = −0.968 ** *p* = 0.000**	***r* = −0.922 ** *p* = 0.000**
Soil Temperature (°C, −20 cm)	***r* = 0.913 ** *p* = 0.000**	***r* = −0.962 ** *p* = 0.000**	***r* = −0.962 ** *p* = 0.000**	***r* = −0.922 ** *p* = 0.000**
Soil Temperature (°C, −50 cm)	***r* = 0.862 ** *p* = 0.000**	***r* = −0.926 ** *p* = 0.000**	***r* = −0.926 ** *p* = 0.000**	***r* = −0.899 ** *p* = 0.000**
Soil Temperature (°C, −1 m)	***r* = 0.749 ** *p* = 0.000**	***r* = −0.821 ** *p* = 0.000**	***r* = −0.821 ** *p* = 0.000**	***r* = −0.836 ** *p* = 0.000**
Precipitation (mm, full-2020–2021)	*r* = −0.162 *p* = 0.484	*r* = 0.079 *p* = 0.733	*r* = 0.079 *p* = 0.733	*r* = 0.047 *p* = 0.840
Precipitation (mm, full-2021–2022)	*r* = −0.230 *p* = 0.316	*r* = 0.148 *p* = 0.522	*r* = 0.148 *p* = 0.522	*r* = 0.088 *p* = 0.703
Precipitation (mm, early spring-2020)	*r* = 0.600 *p* = 0.285	*r* = −0.600 *p* = 0.285	*r* = −0.600 *p* = 0.285	*r* = −0.600 *p* = 0.285
Precipitation (mm, early spring-2021)	*r* = 0.700 *p* = 0.188	*r* = −0.700 *p* = 0.188	*r* = −0.700 *p* = 0.188	*r* = −0.700 *p* = 0.188

3. Results

According to the overall results of this study, although intra-annually displaying similar patterns with each other, the altitude-based LAI values exhibited different courses. Despite this, their values complied with the average LAI values from the LAI-2200C device. In addition, these LAI values did not track the definite increase or decrease trend from the lowest to the highest altitudinal gradients (Figure 4). However, the overall course of their LAI values nearly followed the same pattern. In fact, they almost overlapped with both the air and soil temperatures (Table 2 and Figure 4). On the other hand, the average LT and CO percentages of all the points at those 10 altitudinal gradients showed an approximately symmetrical pattern with the average LAI. Indeed, as if they are inverted, they almost coincide with that overall course of the LAI and the temperature values. Nevertheless, the pattern of the mean GF percentages was obviously different from them, particularly varying with pronounced lower percentages within a relatively narrower range along that temporal extension (Table 2 and Figure 4). Despite all these similarities amongst the intra-annual patterns of these physiological and temperature parameters, there was apparent disparity between the intra-annual patterns of those physiological parameters (Table 2 and Figure 4). Moreover, those intra-annual patterns were disparate from the pattern of the precipitation values along that same temporal extension.

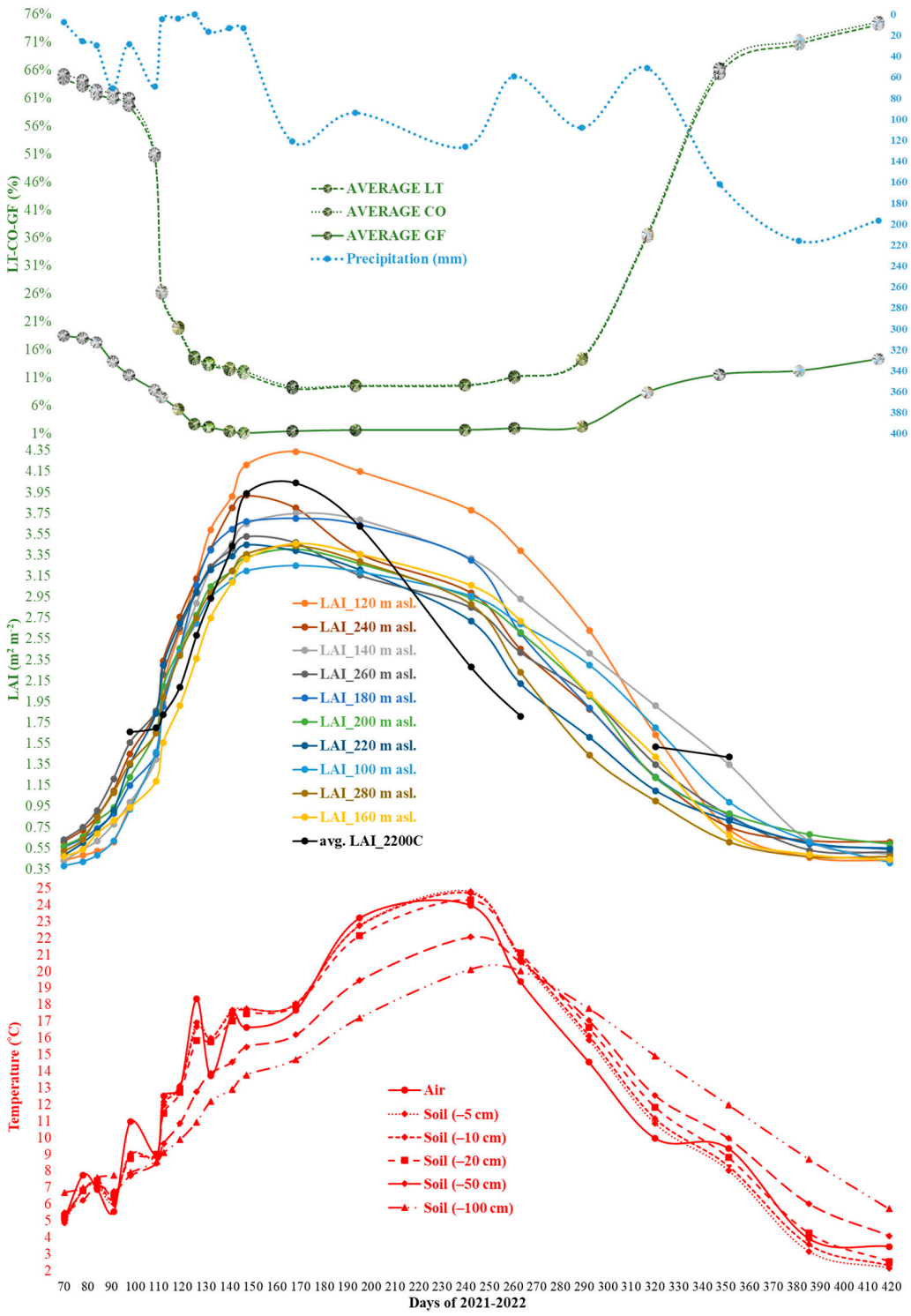


Figure 4. Mean adapted-modified air and soil temperature data (**bottom**), mean LAI data from hemispherical photographs of each altitudinal gradient together with average LAI data from LAI_2200C of all altitudinal gradients (**middle**), and average LT, CO, GF data from hemispherical photographs of all altitudinal gradients together with total precipitation data (**top**) along the monitoring period of 2021–2022.

Table 2. Mean adapted-modified air and soil (−10 cm) temperature, average hemispherical and in-situ device LAI, LT, CO, GF values according to the Date and DOY.

Date	DOY	Mean Air Tempt. (°C)	Mean Soil Tempt. (−10 cm, °C)	Avg. LAI (Hem.) (m^2 m^{-2})	Avg. LAI (2200C) (m^2 m^{-2})	Avg. LT (Hem.) (%)	Avg. CO (Hem.) (%)	Avg. GF (Hem.) (%)
11 March 2021	70	5.1	5.1	0.51		64.4	65.3	18.4
19 March 2021	78	7.8	6.9	0.60		63.2	64.2	18.0
25 March 2021	84	6.9	7.3	0.72		61.6	62.5	17.3
1 April 2021	91	5.6	6.3	0.89		60.9	62.0	13.9
8 April 2021	98	11.0	9.0	1.19	1.66	59.7	61.0	11.5
19 April 2021	109	9.0	8.9	1.59	1.70	50.5	51.1	8.7
22 April 2021	112	12.5	12.0	2.04	1.83	26.0	26.5	7.5
29 April 2021	119	13.0	13.1	2.48	2.09	19.8	20.1	5.3
6 May 2021	126	18.3	16.7	2.88	2.58	14.3	14.7	2.7
12 May 2021	132	13.7	16.0	3.18	2.94	13.2	13.6	2.1
21 May 2021	141	17.4	17.6	3.41	3.44	12.4	12.7	1.4
27 May 2021	147	16.6	17.7	3.56	3.94	11.7	12.2	1.1
17 June 2021	168	17.7	18.1	3.60	4.04	9.0	9.4	1.4
14 July 2021	195	23.2	22.7	3.43	3.63	9.5	9.6	1.6
30 August 2021	242	24.0	24.7	3.08	2.28	9.6	9.7	1.6
20 September 2021	263	19.4	20.9	2.62	1.81	11.2	11.0	1.9
19 October 2021	292	14.5	16.1	2.02		14.2	14.4	2.2
16 November 2021	320	10.0	11.2	1.38	1.52	36.2	36.7	8.4
17 December 2021	351	9.4	8.3	0.85	1.42	65.4	66.3	11.5
20 January 2022	385	3.9	3.6	0.57		70.7	71.4	12.2
23 February 2022	419	3.5	2.3	0.50		74.1	74.7	14.3

At the beginning of the monitoring period (DOY: 70) when the mixed forest stand trees were almost theoretically leafless due to abscission, the highest LAI value of 0.63 m^2 m^{-2} was observed at 260 m asl. However, the lowest LAI value of 0.38 m^2 m^{-2} was observed at the lowest altitudinal gradient, 100 m asl. (Figure 4). During this theoretically leafless period, the reason for the LAI to be slightly more than zero is the last spring's few remaining leaves still existing on the trees, even though they are not photosynthetically active. During that day, the highest LT and CO percentages were about 70% and 71%, respectively, both at 100 m asl., whereas the highest GF percentage was about 25% at 240 m asl. In fact, during the prior week including that day (DOY: 70), the mean air temperature was 5.1 °C and soil temperature rose from 4.9 °C at −5 cm depth to 6.7 °C at −1 m depth (Table 2 and Figure 4). Nonetheless, in one week until then, the total precipitation was 7.2 mm.

Approximately one month later, at the beginning of the leaf unfolding period (DOY: 98) when the first fresh leaves became clearly visible, the highest LAI value of 1.56 m^2 m^{-2} was observed, again at 260 m asl. (Figure 4). However, the lowest LAI value of 0.92 m^2 m^{-2} was observed again at the lowest altitudinal gradient, 100 m asl. During that day, the highest LT, CO, and GF percentages were about 67%, 69%, and 14%, respectively, all at 140 m asl. (Figure 4). Nevertheless, during the prior week, including that day (DOY: 98), the mean air temperature was 11.0 °C and soil temperature declined from 9.0 °C at −5 cm depth to 7.7 °C at −50 cm depth (Table 2 and Figure 4). Nevertheless, in one week until then the total precipitation was 27.2 mm.

Then, 70 days later, at the climax period of leaves (DOY: 168), when the leaves numerically and dimensionally reached their maximum extent, the maximum LAI value of 4.34 m^2 m^{-2} was observed at 120 m asl. (Figure 4). However, the lowest LAI value of 3.25 m^2 m^{-2} was observed again at the lowest altitudinal gradient, 100 m asl. During that day, the lowest LT, CO, and GF percentages were about 6.6%, 6.9%, and 0.5%, respectively, all at 200 m asl. (Figure 4). Indeed, during the prior three weeks, including that day (DOY: 168), the mean air temperature was 17.7 °C and the soil temperature declined from

18.1 °C at −10 cm depth to 14.7 °C at −1 m depth (Table 2 and Figure 4). In the meantime, in the three weeks until then the total precipitation was 117 mm.

Approximately six months later, the theoretical leafless period of leaves (DOY: 351) occurred when the mixed and diverse forest stand trees became almost theoretically leafless due to the latest abscission. During this date, the highest LAI value of 1.35 m^2 m^{-2} was observed at 140 m asl., whereas the lowest LAI value of 0.61 m^2 m^{-2} was observed at the highest altitudinal gradient, 280 m asl. (Figure 4). During that day, the highest LT, CO, and GF percentages were about 73%, 74%, and 14%, respectively, all at the lowest altitudinal gradient, 100 m asl. However, during the prior one month, including that day (DOY: 351), the mean air temperature was 9.4 °C and soil temperature increased from 8.0 °C at −5 cm depth to 12.0 °C at −1 m depth (Table 2 and Figure 4). However, for almost one month until then the total precipitation was 162 mm.

Finally, 68 days later, at the end of the monitoring period (DOY: 419), when the trees shed almost all their leaves before the following leaf budburst stage, the highest LAI value of 0.61 m^2 m^{-2} was observed at 240 m asl. (Figure 4). The lowest LAI value of 0.41 m^2 m^{-2} was observed again at the lowest altitudinal gradient, 100 m asl. During that day, the highest LT, CO, and GF percentages were about 74%, 75%, and 14.3%, respectively, all at the 140 m asl altitudinal gradient (Figure 4). However, during the prior 34 days, including that day (DOY: 419), the mean air temperature was 3.5 °C and soil temperature increased from 2.2 °C at −5 cm depth to 5.7 °C at −1 m depth (Table 2 and Figure 4). In addition, for the 34 days until then the total precipitation was almost 190 mm.

4. Discussion

4.1. Air-Soil Temperature and LAI, LT, CO, GF Correlations (Overall Course and Leaf Phenological Stages)

According to the overall results of this study, even though alternating dependent upon the altitudinal gradients, the overall intra-annual course of the LAI data has almost followed the same pattern as the intra-annual air and soil temperature data (Figure 4). As a matter of fact, there was a high and significant positive correlation (r = 0.894; p = 0.000) between the intra-annual air temperatures and the average LAI data for all the altitudinal gradients (Table 1). The high and positive significant correlations were also valid between the intra-annual temperatures of the soils (Table 1). Indeed, these correlations were primarily significant at the −5 cm (r = 0.930; p = 0.000), −10 cm (r = 0.922; p = 0.000), and −20 cm (r = 0.913; p = 0.000) depths with the intra-annual average LAI data (Table 1). Therefore, these significant correlations have confirmed and supported the direct positive influence of the air-soil temperature on the weekly, monthly, seasonal, and inter-seasonal trend of the LAI data. Relatively recent scientific studies have confirmed the influence of both air and soil temperatures on the seasonal and inter-seasonal dimensional leaf development of the same or similar forest trees [42]. In addition, some of those recent studies have affirmed the influence of the air-soil temperature on their associated LAI and they have suggested similarly high and significant correlations amongst these parameters [13]. On the other hand, again alternating dependent upon the altitudinal gradients, the average LT, CO, GF data have all shown high and significant negative correlations (p = 0.000) with both the air (r = −0.935, −0.935, −0.887 respectively) and upper soil temperatures (r = −0.96 for LT and CO, r = 0.92 for GF; down to first −20 cm depths) (Table 1). Thus, these significant correlations also support the direct negative influence of the air-soil temperature on the weekly, monthly, seasonal, and inter-seasonal trends of the LT, CO, and GF data. The scientific literature has also suggested this situation, confirming the influence of the air-soil temperature on the seasonal and inter-seasonal alterations of these vegetation parameters. Furthermore, the negative correlation between the vegetation

parameter CO and air-soil temperature has been at that high level in the scientific literature. As such, CO estimations can be used for the prediction of in-situ measured air and soil temperatures as well as for predicting some other ecological parameters within the different oak-hornbeam temperate forest types of central Europe [43]. Therefore, any shift in air-soil temperature trend that could be a consequence of forest canopy closure change will most probably affect that forest canopy gap and openness. As such, this shifting temperature will presumably have a direct impact on the associated light penetration through that forest canopy, as indicated in a recent study by [44]. Although an increasing air-soil temperature trend cannot directly be pronounced for the spring, summer, and autumn seasons of the last 10 years (2012–2021, [24]), an apparent increasing trend for the winter air-soil temperature stands out (Figure 5). This increasing trend suggests possible silent warming in winter and associated unexpected earlier budburst dates for the tree leaves. As a matter of fact, earlier budburst dates may either be beneficial in terms of water and soil conservation or be alarming in terms of soil moisture and nutrient depletion within the overall reservoir landscape.

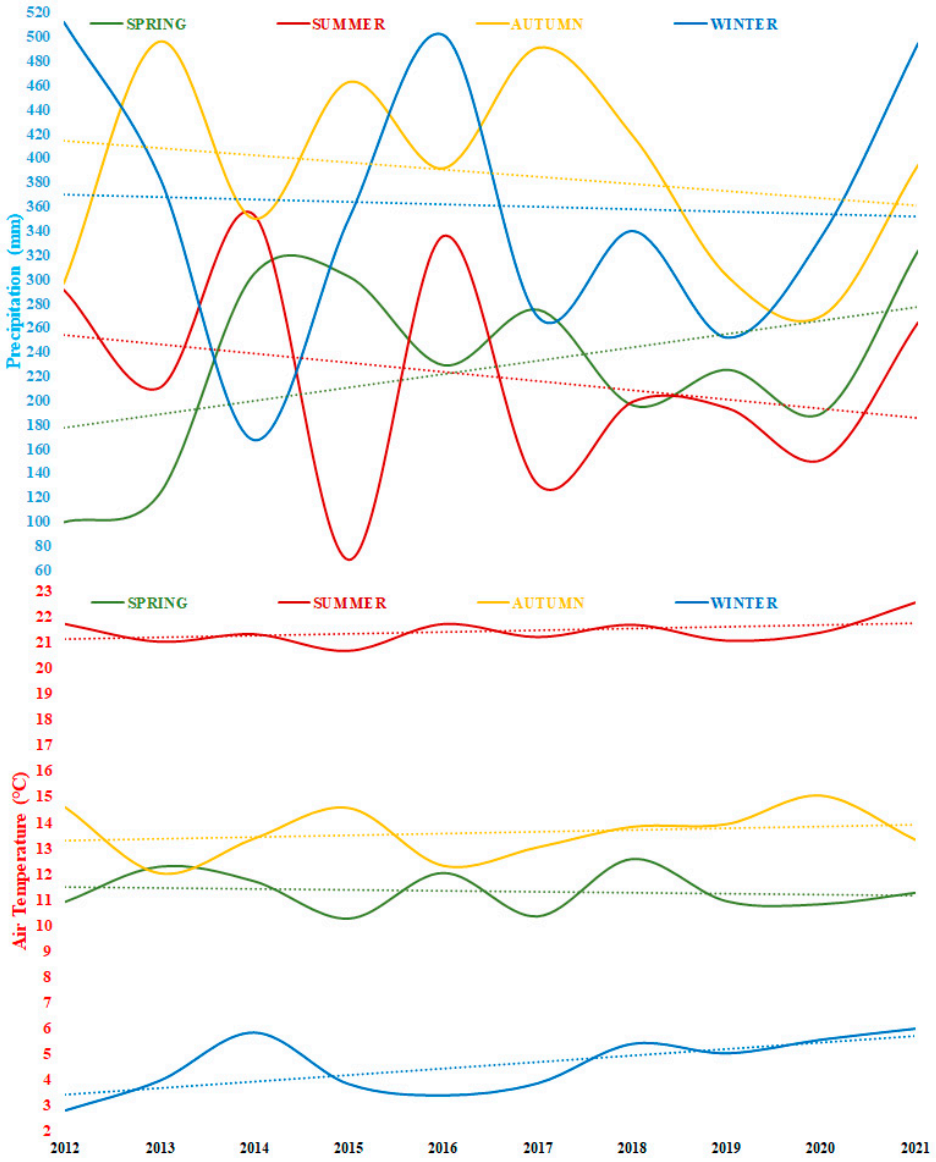


Figure 5. Average adapted-modified seasonal air temperature data (**below**) and average adapted-modified seasonal total precipitation data (**above**) together with their dashed trendlines along the 10 years between 2012 and 2021.

Indeed, depending either on the hemispherical photograph images or on the seasonal course of the LAI, LT, CO, and GF data acquired from their analyses, the leaf budburst and emergence of the first foliage occurred during the second half of March (Table 2 and Figure 4). It occurred principally during late-March when the mean air and soil (−10 cm) temperatures were 6.5 °C and 6.9 °C, respectively (Table 2 and Figure 4). During this leaf budburst and emergence stage, the average LAI increased slightly by 0.38 m^2 m^{-2} (from 0.51 m^2 m^{-2} to 0.89 m^2 m^{-2}), while the average percentages of LT and CO decreased slightly by about 3% (dropping only from 64–65% to 61–62%) (Table 2 and Figure 4). In addition, the average percentage of GF descended by approximately 5% (from 19% to 14%) (Table 2 and Figure 4). On the other hand, in their study of the forest habitats in a national park in north-western Greece, which includes deciduous oak and beech species besides the coniferous trees, the authors of [45] pointed out the period from mid-April to early May for their leaf budburst and first emergence. Considering the altitudinal differences between our study site (~200 m asl.) and their study site (between 400 m and 2637 m asl.), average summer and annual air temperature differences (approximately 4.5 °C for both) between these two sites could have been the main cause for the one-month delay of leaf budburst and emergence dates. Furthermore, in another study of a floodplain forest in south-eastern Czechia at 150 m asl., which is close to the altitude of our study site (~200 m asl.), the authors of [46] indicated almost the same periods and nearly exact dates for the budburst and first emergence of the European hornbeam and then English oak leaves. They also verified almost the same air temperatures (5 to 8 °C) for those dates of leaf budburst and first emergence, coinciding with the results of our study. However, average air and soil (−10 cm) temperatures were 7.4 °C and 9.2 °C, respectively, for the second halves of the March over the last 10 years (2012–2021; [24], Figure 5). Thus, at least for the last 10 years, this situation confirmed that late-March could have been the period of leaf budburst and first emergence within the sample mixed deciduous stand of the reservoir landscape.

The leaf development stage involves the unfolding, expansion, and numerical increase of the deciduous tree leaves. It occurred during the two-month period between early April and early June. This led to the average LAI quadrupling (from 0.89 to 3.56 m^2 m^{-2}) while also leading the average percentages of LT and CO to drop to less than one-fifth (from 61–62% to 12%) (Table 2 and Figure 4). Moreover, this caused the average percentage of GF to drop from 14% to 1% (Table 2 and Figure 4). During this stage, these average LAI values from the hemispherical photographs complied with the average LAI values from the LAI-2200C device (Table 2 and Figure 4). In relation to this, during the same two months period of the leaf development stage, the mean air and soil (−10 cm) temperatures were 13.7 °C and 13.6 °C, respectively, which were very close to the average annual air and soil temperatures (both 13.3 °C). Nevertheless, they were around two-fold of those during the lead budburst and emergence stage (6.5 °C for air and 6.9 °C for −10 cm soil) (Table 2 and Figure 4). Correspondingly, in their study site within the mature and mixed temperate forest of Switzerland involving diverse tree species, including oaks, hornbeams, and beeches, as in our study site, the authors of [47] determined early May as the beginning of the leaf development stage for the same year (2021) of their study. According to their study, during the spring of 2021, the mean air temperature in their study site (550 m asl.) was 7.7 °C. It was about 3.6 °C lower than the mean spring temperature (~11.3 °C for the year 2021) of our study site. Therefore, this air temperature difference with our study site corresponds to the lapse rate (about 1.0 °C/100 m) when compared to the altitudinal difference with our study site (~200 m asl.). Confirming this correspondence, the mean annual air temperature within their study site was 9.6 °C, which reveals almost the same difference (3.7 °C) compared to the mean annual air temperature (~13.3 °C) of our study site. Compared with our study site, it also revealed their one-month delay for the beginning and

duration period of the leaf development stage. On the other hand, the long-term average air and soil (−10 cm) temperatures for the two-month period of our leaf development stage (April and May) were 13.3 °C and 15.6 °C, respectively, over the last 10 years (2012 and 2021; [24], Figure 5). Therefore, it is suggested that both the air-soil temperature and the duration period of leaf development have not changed much during that last decade. The authors of [48] also remarked on the joint elevation and topography-driven maximum temperature for the best prediction of the plant community composition, particularly for the understory plant species.

The stationary leaf stage is when both the size and number of the tree leaves gain their maximum level. This was achieved during early June and lasted two-and-a half month until mid-August. During this stationary stage, the average LAI fluctuated within a narrow range between 3.43 and 3.60 m^2 m^{-2} (Table 2 and Figure 4). These values again complied with the average LAI values from the LAI-2200C device (Table 2 and Figure 4). However, during this stationary stage, the average percentages of LT and CO were both within the relatively narrow ranges between 9 and 12%, whereas the average percentage of GF was within a narrow range between 1 and 2% (Table 2 and Figure 4). Hence, during the same two-and-a half month period of stationary leaf stage, the mean air and soil (−10 cm) temperatures were 22.5 and 22.6 °C, respectively. Thus, they were very close to the average whole summer air and soil temperatures (22.6 and 22.9 °C, respectively; Table 2 and Figure 4). In their study of a temperate deciduous forest composed of mainly sessile oaks and European hornbeams, such as in our study, the authors of [49] monitored their leaf phenology at a similar altitude (103 m asl.) in western France. In that study, both the mean summer and annual air temperatures were quite consistent with those in our study site. They determined that the mean LAI achieved its maximum values during early June. Furthermore, their maximum LAI lasted until nearly the end of summer (late-August), almost the same duration defined in our study for the stationary leaf stage (Table 2 and Figure 4).

The deciduous leaf senescence stage involves the period from the end of the stationary leaf stage to the leaf discoloration stage, to the leaf fading, to the leaf fall, and until the theoretical leafless stage. It lasted approximately for the three-and-a half month period from mid-August until the end of November. During this leaf senescence stage, the average LAI dropped from 3.43 m^2 m^{-2} down to 0.85 m^2 m^{-2} (Table 2 and Figure 4). These values also complied with the average LAI values from the LAI-2200C device (Table 2 and Figure 4). In fact, depending on the meta-analysis of autumn phenology studies, the authors of [50] referred to almost the same period as our study for the autumn senescence of the deciduous trees within the closer latitudes of the northern hemisphere. During this leaf senescence stage, conversely, our average percentage of LT climbed from 9% up to 65% and similarly average percentage of CO ascended from 10% up to 66% (Table 2 and Figure 4). The average percentage of GF increased from 1% up to 12% (Table 2 and Figure 4). Nonetheless, during this three-and-a half month senescence stage, the mean air and soil (−10 cm) temperatures were 14.8 °C and 15.9 °C, respectively. Hence, they were close to the long-term average air and soil (−10 cm) temperatures (14.8 and 17.6 °C) for the three-and-a half month period of leaf senescence stage (from mid-August to the end of November) during the last 10 years (2012 and 2021; [24], Figure 5). Thus, it suggested that both the air-soil temperature and the duration period of leaf senescence had not changed much throughout that last decade. However, a European study on European beeches and pedunculate oaks, two of the dominant temperate tree species in Europe, ref. [51] suggested late-September and early-October for the senescence of European beeches and pedunculate oaks. In addition, they indicated that their senescence had been delayed due to global warming, particularly during the last half of the long-term period between 1951 and 2013.

The theoretical leafless stage is when the deciduous trees are almost bare without leaves or with their last few remaining dry leaves palely hanging on their branches. This theoretical leafless stage was reached during early December and it lasted three months throughout the whole winter until the end of February. Presumably, this theoretical leafless stage is followed by the first formation of the next year's buds, and this proceeds during the first half of March. Indeed, during this theoretical leafless stage, the average LAI declined from 0.85 m^2 m^{-2} down to 0.50 m^2 m^{-2}. During this theoretical leafless stage, conversely, the average percentages of LT and CO were approximately within their high ranges, between 65 and 75%, whereas the average percentage of GF was within a narrow range between 12 and 14%. (Table 2 and Figure 4). As a matter of fact, based on the review of scientific studies, depending upon the ground-based measurements of LAI, the authors of [52] indicated that the LAI of a European forest that involves similar deciduous trees as in our study had fallen below 1 m^2 m^{-2}, particularly after late-October and early-November. Their study confirmed the validity of a one-month delay for the initiation of a theoretical leafless stage, such as previous stages in Europe when compared with our study. On the other hand, during that winter (December 2021 and January and February 2022) in our study, the mean air and (−10 cm) soil temperatures were 5.0 and 4.1 °C, respectively (Table 2 and Figure 4). Therefore, they were close to the long-term (10 years between 2012 and 2021; [24], 2022, Figure 5) average winter air and soil (−10 cm) temperatures (4.6 and 5.2 °C, respectively) (Table 2 and Figure 4). Nevertheless, silent warming can be seen for the winter air temperature within the reservoir landscape.

4.2. Precipitation and LAI, LT, CO, GF Correlation (Overall Course and Leaf Phenological Stages)

On the other hand, the authors of [53] suggested the positive influence of the preceding year's summer precipitation, rather than the air temperature, on the total number of the European beech leaves per ground area within the forests of central Germany. Indeed, in our study, the correlation between the periodic total precipitations and the LAI data was negative and relatively insignificant ($r = -0.230$; $p = 0.316$, Table 1). This insignificant correlation indicated the weak influence of precipitation on the development of LAI when compared to the air-soil temperature during the intervals between those field visits. The same insignificant situation was valid but reversed for the other canopy parameters. Thus, positive correlation coefficients (r) were valid with 0.148, 0.148, and 0.088 for the LT, CO, and GF, respectively (Table 1). On the other hand, in their study for the forests in the Flanders region of Belgium, the authors of [54] insisted on the previous year's higher summer precipitation as one of the causes for the decrement in the LAI within a beech stand. However, they indicated a positive correlation between the previous year's spring precipitation and the LAI within an oak stand. For our study, there was a positive yet insignificant correlation ($r = 0.600$; $p = 0.285$, Table 1) between the previous year's early spring (early March to early April of 2020) precipitation and the LAI data of that term (2021). Nonetheless, any apparent correlation was not valid for the whole spring season and even for that whole year ($r = -0.162$; $p = 0.484$, Table 1). Moreover, insignificant negative correlation coefficients (r) were valid for the other canopy parameters, LT, CO, and GF (−0.600 for all, Table 1), in terms of the previous year's early spring precipitation. However, this situation was not valid for that whole year (r = 0.079, 0.079, 0.047, respectively, Table 1). Nevertheless, the increasing trend of the spring precipitation during the last 10 years (Figure 5) may possibly trigger the increment of the annual maximum LAI. Similarly, for some of the dominant tree and shrub species within the central Loess Plateau of China, the study by [55] also remarked on the correlation of the annual maximum LAI with the precipitation gradients along the years.

5. Conclusions

Based on the continuous intra-annual monitoring and analyses of the deciduous tree canopy parameters, it can certainly be concluded that these parameters, and accordingly the phenological stages, displayed definite patterns throughout the monitoring year. However, annual patterns of these canopy parameters followed an overlapping or symmetrical course with the annual air-soil temperature patterns. On the other hand, their overlapping or symmetrical course was not valid for the precipitation pattern. Nevertheless, highly significant positive or negative correlations between these canopy parameters and those air-soil temperature data also confirmed these similarities. Hence, the determinant role of air-soil temperatures on these canopy parameters, particularly during the turning points of the seasons and associated phenological periods, was one of the substantial consequences of this study. Therefore, any shifting or fluctuation in the air-soil temperature averages may lead to the shifting in tree phenology and may accordingly induce essential changes for the deciduous tree canopy ecophysiology within the forest ecosystem. For this reason, our study will be able to serve as a basis for further scenario analyses, either on possible changing air-soil temperatures or on precipitation regime irregularities. Indeed, these changes and irregularities may influence both the surface and soil water and may affect the overall phenology and eco-physiology of the reservoir landscape. Moreover, principally during the transitions between dormancy and growing seasons, these climate-induced possible phenological and eco-physiological alterations may directly or indirectly influence tree photosynthesis. Hence, any change in the photosynthetic activity of the trees will thereby have impacts on the productivity of the entire forest ecosystem within the reservoir landscape.

On the other hand, these canopy parameters have not displayed any definite ascending or descending trend from the lowest to the highest altitudinal gradient. Nevertheless, the vertical variance in the composition and density of the forest tree species was also determinant on these canopy parameters. However, this situation might alter as one of the consequences of eventual temperature-moderating impact of the dam reservoir water by humidifying the air. Furthermore, maintaining both the existence and diversity of the mixed deciduous trees composed of four species is crucial. In fact, their diversity supports and secures the preservation and sustainability of the dam reservoir water not only within the riparian zone but also within the entire reservoir landscape. Consequently, land use and forest management plans, proposals, and practices should primarily focus on the diversity of vegetation, and water and soil conservation. For this purpose, on-site monitoring and tracking by means of ground and satellite images should be carried out continuously within the entire reservoir landscape. In addition, the monitoring and analyses of tree phenology and canopy parameters should constantly be conducted within the forest ecosystems.

Author Contributions: Conceptualization, M.Ö. and T.B.; methodology, M.Ö.; software, M.Ö. and T.B.; validation, M.Ö., T.B. and A.V.A.; formal analysis, M.Ö.; investigation, M.Ö. and T.B.; resources, M.Ö.; data curation, M.Ö., T.B. and A.V.A.; writing—original draft preparation, M.Ö.; writing—review and editing, M.Ö., T.B. and A.V.A.; visualization, M.Ö. and T.B.; supervision, M.Ö.; project administration, M.Ö. and T.B.; funding acquisition, M.Ö. All authors have read and agreed to the published version of the manuscript.

Funding: This research received no external funding.

Institutional Review Board Statement: The Department of Landscape Architecture at the Graduate School of Bartın University reviewed this study and approved with the number of 2024/8.

Data Availability Statement: The data and material of this work have not been shared publicly elsewhere and therefore can only be available after it is published.

Acknowledgments: The data of this study is from the master thesis of the second author, that was submitted to the Department of Landscape Architecture at the Graduate School of Bartın University and approved with the date of 1 March 2024 and number of 2024/8. Therefore, the authors of this study owe the institute a dept of gratitude for all those supports. Forest Engineers Hasan Güneş and Serkan Bulut are gratefully acknowledged for their complimentary support during the field works of this study. In addition, we would like to credit Turkish State Meteorological Service, which provided the meteorological data, and Turkish General Directorate of Forestry which shared the forest management plans and maps with us. Above all, we would like to appreciate our Bartın University which continuously encouraged our studies with financial and moral supports.

Conflicts of Interest: The authors declare that they have no known competing financial interests or personal relationships that could have appeared to influence the work reported in this paper.

References

1. Marsh, W.M. *Landscape Planning: Environmental Applications*, 5th ed.; John Wiley & Sons, Inc.: Hoboken, NJ, USA, 2010.
2. Turner, M.G.; Gardner, R.H. *Landscape Ecology in Theory and Practice; Pattern and Process*, 2nd ed.; Springer Science + Business Media LLC: New York, NY, USA, 2015.
3. Öztürk, M.; Copty, N.K. Landscape Planning for Sustainable Groundwater Resources. In *New Approaches to Spatial Planning and Design; Planning, Design and Applications*; Özyavuz, M., Ed.; Peter Lang Publications: Berlin, Germany, 2019; Chapter 23; pp. 325–332. [CrossRef]
4. Chang, M. *Forest Hydrology: An Introduction to Water and Forests*, 2nd ed.; CRC, Taylor and Francis: Boca Raton, FL, USA, 2006.
5. Bonan, G. *Ecological Climatology: Concepts and Applications*, 3rd ed.; Cambridge University Press: New York, NY, USA, 2016.
6. Forman, R.T.T. *Land Mosaics; The Ecology of Landscapes and Regions*; Cambridge University Press: Cambridge, UK, 1995.
7. Wang, F.; Wang, X.; Zhao, Y.; Yang, Z. Temporal variations of NDVI and correlations between NDVI and hydro-climatological variables at Lake Baiyangdian, China. *Int. J. Biometeorol.* **2014**, *58*, 1531–1543. [CrossRef] [PubMed]
8. Portillo-Quintero, C.; Sanchez-Azofeifa, A.; Calvo-Alvarado, J.; Quesada, M.; do Espirito Santo, M.M. The role of tropical dry forests for biodiversity, carbon and water conservation in the neotropics: Lessons learned and opportunities for its sustainable management. *Reg. Environ. Change* **2015**, *15*, 1039–1049. [CrossRef]
9. Yang, H.; Wang, J.; Xiao, W.; Lu, F.; Wang, Y.; Jarsjö, J. Relationship between hydroclimatic variables and reservoir wetland landscape pattern indices: A case study of the Sanmenxia Reservoir wetland on the Yellow River, China. *J. Earth Syst. Sci.* **2020**, *129*, 83. [CrossRef]
10. Slimane, A.B.; Raclot, D.; Evrard, O.; Sanaa, M.; Lefevre, I.; Bissonais, Y.L. Relative contribution of rill/interrill and gully/channel erosion to small reservoir siltation in Mediterranean environments. *Land Degrad. Dev.* **2016**, *27*, 785–797. [CrossRef]
11. Zhirnova, D.F.; Belokopytova, L.V.; Meko, D.M.; Babushkina, E.A.; Vaganov, E.A. Climate change and tree growth in the Khakass-Minusinsk Depression (South Siberia) impacted by large water reservoirs. *Sci. Rep.* **2021**, *11*, 14266. [CrossRef]
12. Panyushkina, I.P.; Meko, D.M.; Macklin, M.G.; Toonen, W.H.J.; Mukhamadiev, N.S.; Konovalov, V.G.; Ashikbaev, N.Z.; Sagitov, A.O. Runoff variations in Lake Balkhash Basin, Central Asia, 1779–2015, inferred from tree rings. *Clim. Dyn.* **2018**, *51*, 3161–3177. [CrossRef]
13. Öztürk, M.; Bolat, İ.; Ergün, A. Influence of air–soil temperature on leaf expansion and LAI of *Carpinus betulus* trees in a temperate urban forest patch. *Agric. For. Meteorol.* **2015**, *200*, 185–191. [CrossRef]
14. Song, Z.; Liang, S.; Feng, L.; He, T.; Song, X.-P.; Zhang, L. Temperature changes in Three Gorges Reservoir Area and linkage with Three Gorges Project. *J. Geophys. Res. Atmos.* **2017**, *122*, 4866–4879. [CrossRef]
15. Kellogg, C.H.; Zhou, X. Impact of the construction of a large dam on riparian vegetation cover at different elevation zones as observed from remotely sensed data. *Int. J. Appl. Earth Obs. Geoinf.* **2014**, *32*, 19–34. [CrossRef]
16. Perry, D.A.; Oren, R.; Hart, S.C. *Forest Ecosystems*, 2nd ed.; The Johns Hopkins University Press: Baltimore, MD, USA, 2008.
17. Waring, R.H.; Running, S.W. *Forest Ecosystems: Analysis at Multiple Scales*, 3rd ed.; Elsevier Academic Press: London, UK, 2007.
18. Bao, J.; Li, J.; Wang, G.; Tang, Z.; Zhi, J. Branch growth, leaf canopies and photosynthetic responses of *Zizyphus jujube* cv. "Huizao" to nutrient addition in the arid areas of Northwest China. *Diversity* **2022**, *14*, 914. [CrossRef]
19. Sun, G.; Wei, X.; Hao, L.; Sanchis, M.G.; Hou, Y.; Yousefpour, R.; Tang, R.; Zhang, Z. Forest hydrology modeling tools for watershed management: A review. *For. Ecol. Manag.* **2023**, *530*, 120755. [CrossRef]
20. Leblanc, S.G.; Fournier, R.A. Measurement of forest structure with hemispherical photography. In *Hemispherical Photography in Forest Science: Theory, Methods, Applications*; Fournier, R.A., Hall, R.J., Eds.; Springer Science+Business Media, B.V.: Dordrecht, The Netherlands, 2017; pp. 53–83. [CrossRef]
21. Bequet, R.; Campioli, M.; Kint, V.; Vansteenkiste, D.; Muys, B.; Ceulemans, R. Leaf area index development in temperate oak and beech forests is driven by stand characteristics and weather conditions. *Trees* **2011**, *25*, 935–946. [CrossRef]

22. Öztürk, M.; Ağırtaş, L. Canopy parameters for tree and shrub species compositions in differently intervened land uses of an urban park landscape. *Build. Environ.* **2021**, *206*, 108340. [CrossRef]
23. Öztürk, M.; Gökyer, E. Spatio-temporal variation of forest trees surrounding the Bartın-Kirazlıköprü dam reservoir: Landscape evaluation around the concept of tourism and recreation. In Proceedings of the 1st International Conference on Tourism and Architecture, Karabük, Türkiye, 24–27 October 2018.
24. TSMS (Turkish State Meteorological Service). *Meteorological Data of Bartın (Türkiye) Meteorology Station*; TSMS: Ankara, Türkiye, 2022.
25. Atalay, İ. *Climate Atlas of Türkiye*; İnkılâp Bookstore Press: İstanbul, Türkiye, 2011. (In Turkish)
26. TGDF (Turkish General Directorate of Forestry). *Forest Management Plans (2006 and 2021) of Yenihan Sub-District of Bartın Forestry Administration Affiliated to the Zonguldak Regional Forest Directorate*; TGDF: Ankara, Türkiye, 2021.
27. TMAF (Turkish Ministry of Agriculture and Forestry). *Digital Soil Maps of Bartın Stream Watershed*; TMAF: Ankara, Türkiye, 2005.
28. TGDMER (Turkish General Directorate of Mineral Exploration and Research). *Digital Geological Maps of Zonguldak E-29 Section*; TGDMER: Ankara, Türkiye, 2007.
29. Davis, P.H. *Flora of Turkey and the Aegean Islands*; Edinburgh University Press: Edinburgh, UK, 1982; Volumes I, II and VII.
30. Yaltırık, F. *Dendrology*, 2nd ed.; İstanbul University, Faculty of Forestry Press: İstanbul, Türkiye, 1993; Volume II, (Angiospermae; I. Amentiferae-II. Floriferae: Apatalae). (In Turkish)
31. Bréda, N.; Granier, A. Intra- and interannual variations of transpiration, leaf area index and radial growth of a sessile oak stand (*Quercus petraea*). *Ann. For. Sci.* **1996**, *53*, 521–536. [CrossRef]
32. Ducousso, A.; Guyon, J.P.; Krémer, A. Latitudinal and altitudinal variation of bud burst in western populations of sessile oak (*Quercus petraea* (Matt) Liebl). *Ann. For. Sci.* **1996**, *53*, 775–782. [CrossRef]
33. Atalay, İ. *Ecosystem Ecology and Geography*; Meta Press and Printing: Bornova, İzmir, Türkiye, 2008; Volume II. (In Turkish)
34. Çepel, N. *Landscape Ecology*; İstanbul University, Faculty of Forestry Press: İstanbul, Türkiye, 1994. (In Turkish)
35. Anşin, R.; Özkan, Z.C. *Seed Plants (Spermatophyte), Ligneous Taxon*; Karadeniz Technical University, Faculty of Forestry Press: Trabzon, Türkiye, 1997. (In Turkish)
36. Saatçioğlu, F. Silviculture I. In *Biological Fundamentals and Principles of Silviculture*, 2nd ed.; İstanbul University, Faculty of Forestry Press: İstanbul, Türkiye, 1976. (In Turkish)
37. Schleppi, P.; Conedera, M.; Sedivy, I.; Thimonier, A. Correcting non-linearity and slope effects in the estimation of the leaf area index of forests from hemispherical photographs. *Agric. For. Meteorol.* **2007**, *144*, 236–242. [CrossRef]
38. Nobis, M.; Hunziker, U. Automatic thresholding for hemispherical canopy photographs based on edge detection. *Agric. For. Meteorol.* **2005**, *128*, 243–250. [CrossRef]
39. Chen, J.M.; Cihlar, J. Quantifying the effect of canopy architecture on optical measurements of leaf area index using two gap size analysis methods. *IEEE Trans. Geosci. Remote Sens.* **1995**, *33*, 777–787. [CrossRef]
40. Barry, R.G. *Mountain Weather and Climate*, 3rd ed.; Cambridge University Press: New York, NY, USA, 2008.
41. Devore, J.; Farnum, N. *Applied Statistics for Engineers and Scientists*, 1st ed.; Duxbury Press: Grove, CA, USA, 1999.
42. Urban, J.; Bednářová, E.; Plichta, R.; Gryc, V.; Vavrčík, H.; Hacura, J.; Fajstavr, M.; Kučera, J. Links between phenology and ecophysiology in a European beech forest. *iForest-Biogeosci. For.* **2014**, *8*, 438–447. [CrossRef]
43. Hederová, L.; Macek, M.; Wild, J.; Brůna, J.; Kašpar, V.; Klinerová, T.; Kopecký, M. Ecologically relevant canopy openness from hemispherical photographs. *Agric. For. Meteorol.* **2023**, *330*, 109308. [CrossRef]
44. Kašpar, V.; Hederová, L.; Macek, M.; Müllerová, J.; Prošek, J.; Surový, P.; Wild, J.; Kopecký, M. Temperature buffering in temperate forests: Comparing microclimate models based on ground measurements with active and passive remote sensing. *Remote Sens. Environ.* **2021**, *263*, 112522. [CrossRef]
45. Stagakis, S.; Markos, N.; Vanikiotis, T.; Levizou, E.; Kyparissis, A. Multi-year monitoring of deciduous forests ecophysiology and the role of temperature and precipitation as controlling factors. *Plants* **2022**, *11*, 2257. [CrossRef] [PubMed]
46. Nezval, O.; Krejza, J.; Světlík, J.; Šigut, L.; Horáček, P. Comparison of traditional ground-based observations and digital remote sensing of phenological transitions in a floodplain forest. *Agric. For. Meteorol.* **2020**, *291*, 108079. [CrossRef]
47. Zahnd, C.; Arend, M.; Kahmen, A.; Hoch, G. Microclimatic gradients cause phenological variations within temperate tree canopies in autumn but not in spring. *Agric. For. Meteorol.* **2023**, *331*, 109340. [CrossRef]
48. Macek, M.; Kopecký, M.; Wild, J. Maximum air temperature controlled by landscape topography affects plant species composition in temperate forests. *Landscape Ecol.* **2019**, *34*, 2541–2556. [CrossRef]
49. Soudani, K.; Delpierre, N.; Berveiller, D.; Hmimina, G.; Pontailler, J.-Y.; Seureau, L.; Vincent, G.; Dufrêne, É. A survey of proximal methods for monitoring leaf phenology in temperate deciduous forests. *Biogeosciences* **2021**, *18*, 3391–3408. [CrossRef]
50. Gill, A.L.; Gallinat, A.S.; Sanders-DeMott, R.; Rigden, A.J.; Short Gianotti, D.J.; Mantooth, J.A.; Templer, P.H. Changes in autumn senescence in northern hemisphere deciduous trees: A meta-analysis of autumn phenology studies. *Ann. Bot.* **2015**, *116*, 875–888. [CrossRef]

51. Chen, L.; Huang, J.-G.; Ma, Q.; Hänninen, H.; Tremblay, F.; Bergeron, Y. Long-term changes in the impacts of global warming on leaf phenology of four temperate tree species. *Global Change Biol.* **2019**, *25*, 997–1004. [CrossRef]
52. Bréda, N.J.J. Ground-based measurements of leaf area index: A review of methods, instruments and current controversies. *J. Exp. Bot.* **2003**, *54*, 2403–2417. [CrossRef]
53. Meier, I.C.; Leuschner, C. Leaf size and leaf area index in *Fagus sylvatica* forests: Competing effects of precipitation, temperature, and nitrogen availability. *Ecosystems* **2008**, *11*, 655–669. [CrossRef]
54. Bequet, R.; Kint, V.; Campioli, M.; Vansteenkiste, D.; Muys, B.; Ceulemans, R. Influence of stand, site and meteorological variables on the maximum leaf area index of beech, oak and Scots pine. *Eur. J. For. Res.* **2012**, *131*, 283–295. [CrossRef]
55. Zhang, Y.; Huang, M.; Lian, J. Spatial distributions of optimal plant coverage for the dominant tree and shrub species along a precipitation gradient on the central Loess Plateau. *Agric. For. Meteorol.* **2015**, *206*, 69–84. [CrossRef]

Disclaimer/Publisher's Note: The statements, opinions and data contained in all publications are solely those of the individual author(s) and contributor(s) and not of MDPI and/or the editor(s). MDPI and/or the editor(s) disclaim responsibility for any injury to people or property resulting from any ideas, methods, instructions or products referred to in the content.